ADVANCED MATERIALS

Supporting Information

for *Adv. Mater.*, DOI: 10.1002/adma.201705791

Graphene–Graphene Interactions: Friction, Superlubricity, and Exfoliation

*Robert C. Sinclair, James L. Suter, and Peter V. Coveney**

Graphene-graphene interactions: friction, superlubricity and exfoliation
— Supporting Information —

Robert C. Sinclair, James L. Suter, Peter V. Coveney

November 27, 2017

In this supplementary information, we provide additional discussions of the methods and results of our study. This includes clarifying details of the simulations, justifications for our methods and some more points of interest.

CONTENTS

I. ADDITIONAL INFORMATION FROM DESIGNING GRAFF

To construct our new GraFF forcefield, we firstly identified the best existing forcefields for simulating the adsorption of graphene for simulating. The results of the adsorption energies of a graphite sheet using established forcefields (OPLS, AMBER, COMPASS and Driedling) along with comparisons to experiment and DFT simulations are shown in Figure S1 (and Table III in the main text)[1–5]. Both AMBER and Dreidling forcefields overestimate the adsorption energy and layer spacing (and are outside of the experimental region); these forcefields were therefore discounted on this basis for the GraFF forcefield.

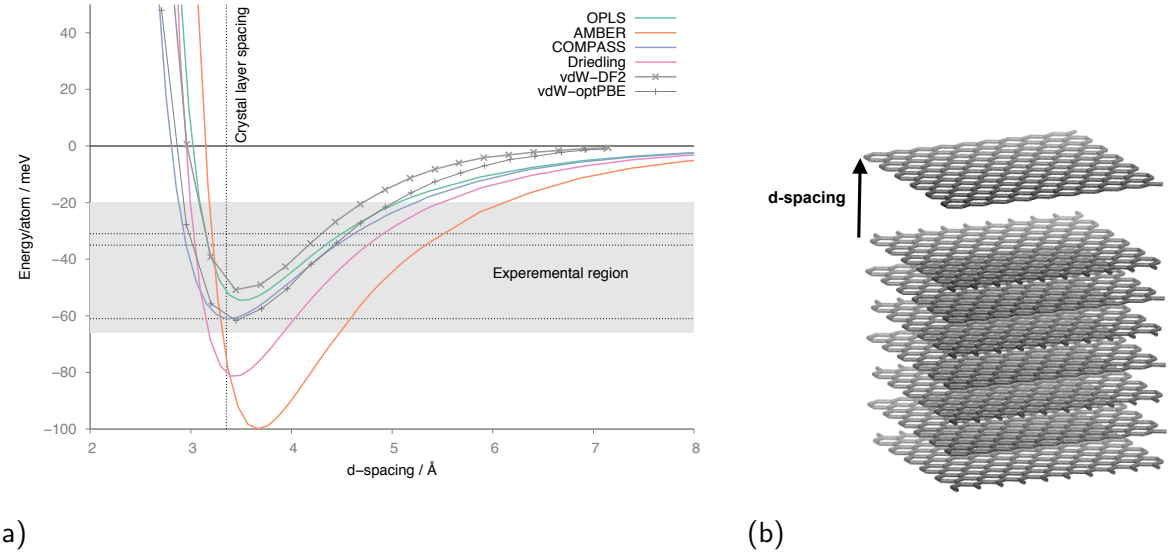

FIG. S1: (a) shows comparison of the exfoliation energies calculated using existing forcefields (OPLS[2], AMBER[1], COMPASS[4] and Dreiding[3]), DFT calculations (vdW-DF2 and vdW-optPBE[5]) and experiment[6–8]. For exact values and references see Table III in the main text. The experimental region is very large; dashed lines represent the values reported by individual experiments. Classical forcefields predict a much larger long range interaction. (b) shows the adsorption energy simulation setup.

Previous studies, for both graphene and clay cases, suggest that the most facile method of exfoliation is via a sliding mechanism[9,10]. Sliding two AB stacked graphene sheets past each other along the vectors shown in Figure S2a using established MD forcefields[1–4] and the DFT simulation of Gao *et al.*[11] DFT are shown in Figure S2.

Using GraFF the energies are shown in Figure S3. The most important energy barrier to reproduce is the smallest peak in the armchair sliding experiment, i.e. Figure S3b.

Figure S5 illustrates the importance of capturing the smallest peak in Figure S3b. A

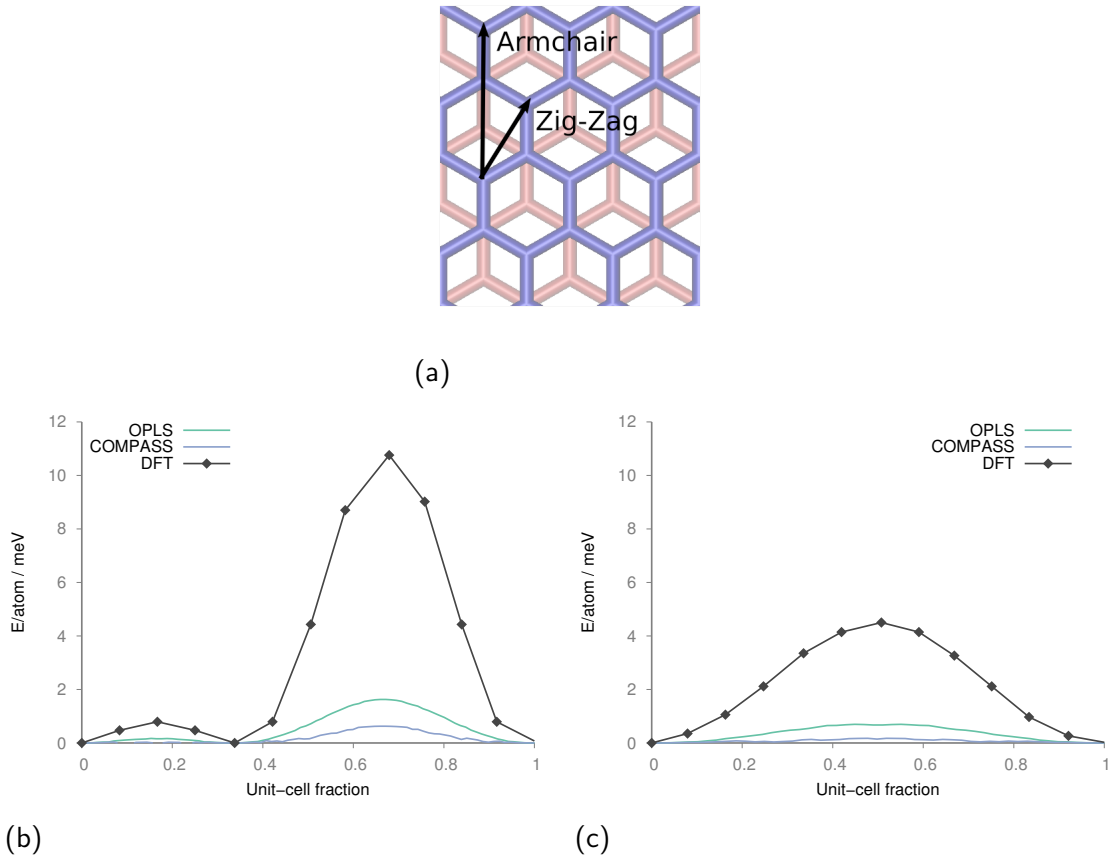

FIG. S2: Sliding two sheets of graphene past each other using different forcefields. (a) shows the vector along which the top sheet (blue) slides: (b) armchair; (c) zig-zag. The key energy barrier to sliding is identified as the smaller peak in (b) as flakes can zig-zag past each other without encountering a higher peak.

flake can slide over another in the armchair pattern or zig-zag pattern shown in Figure S5a without encountering any higher energy barriers. By symmetry each segment in the paths shown in Figure S5a has the same energy barrier associated with it, shown in Figure S5b. The second peak in Figure S3b is due to completely overlapping sheets, i.e. AA stacking; this is much higher in energy and therefore unlikely to be explored.

The parameters used in GraFF — described by equations 1 and 2 in the main article — are described in the schematic shown in Figure S6. The forces on C_1 and C_2 are:

$$\begin{aligned} \mathbf{F}_{C_2} &= \mathbf{F}_{kernel} + \mathbf{F}_{angle}, \\ \mathbf{F}_{C_1} &= -\mathbf{F}_{C_2}, \end{aligned} \tag{1}$$

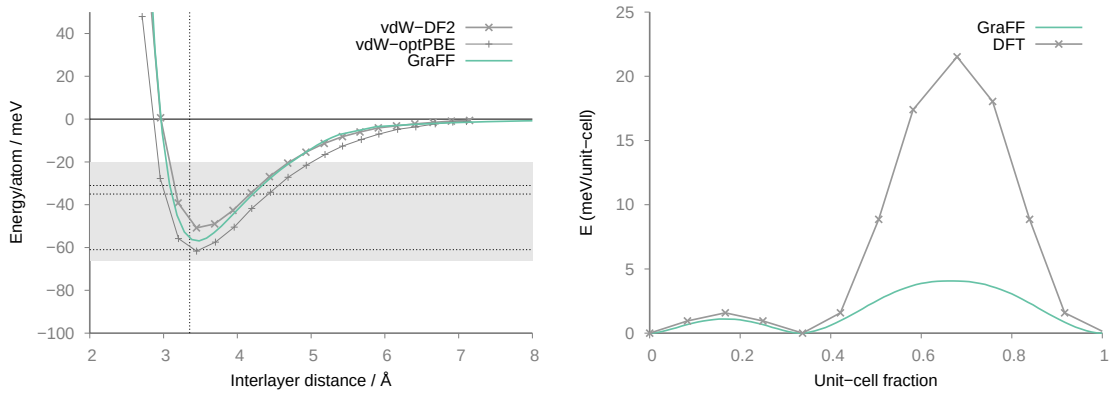

(a) (b)

FIG. S3: Energies of (a) graphene adsorption and (b) sliding sheets using the new forcefield GraFF. These graphs can be compared with figures S1 and S2. The dotted lines in (a) represent different experimentally found adsorption energies; see Table III in the main article.

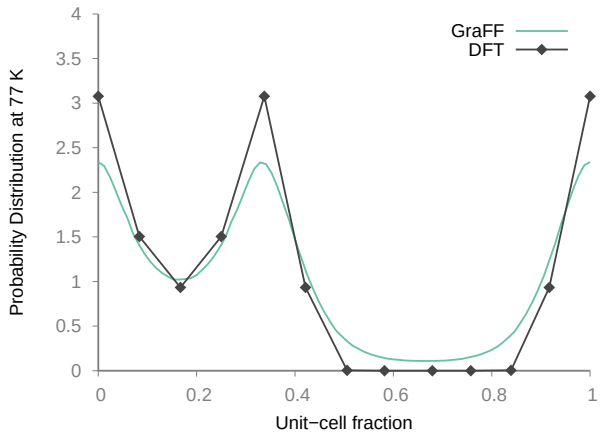

FIG. S4: To give some indication of the equilibrium populations of two flakes along the armchair vector in Figure S2a we use the relation $P = exp(-\Delta E/k_B T)$ where ΔE is given in Figure S3b. This shows that GraFF provides a sufficient energy penalty at unit-cell fraction between $0.45 - 0.85$, leading to a very low population at these positions, matching the DFT results.

where:

$$\begin{aligned} \mathbf{F}_{kernel} &= \frac{\partial}{\partial r_{C_1C_2}} V(r_{C_1C_2}, \theta) \cdot \hat{\mathbf{r}}_{C_1C_2}, \\ \mathbf{F}_{angle} &= \frac{\partial}{\partial \theta} V(r_{C_1C_2}, \theta) \cdot \hat{\mathbf{r}}_{tan}, \\ \hat{\mathbf{r}}_{tan} &= (\hat{\mathbf{r}}_{C_1C_2} \times \hat{\mathbf{r}}_{C_1C_R}) \times \hat{\mathbf{r}}_{C_1C_2}. \end{aligned} \tag{2}$$

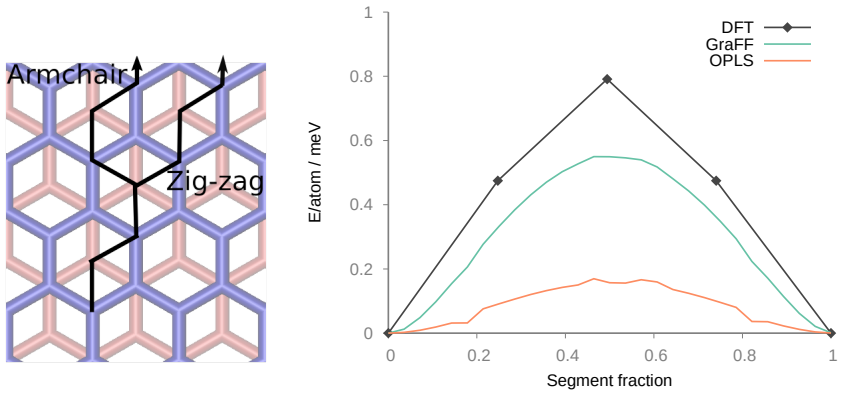

(a) (b)

FIG. S5: Minimum energy pathways for a graphene sheet sliding over another. Each line segment in (a) has the same energy barrier, shown in (b).

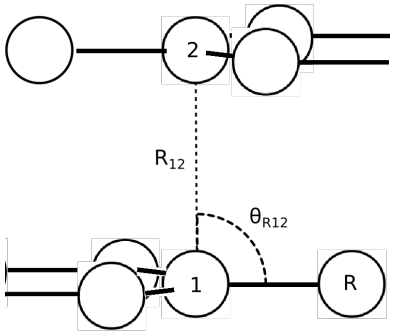

FIG. S6: Schematic of the parameters used in the 3-body potential of GraFF. See equations 1 and 2 in the main text.

Similar to many forcefields, GraFF cannot represent chemical reactions, but we expect it to be transferable to many situations were graphene and graphene oxide are involved.

II. DISCUSSION OF THE PROPULSION IMPLEMENTATION

The propulsion in Feng *et al.*'s original experiment is provided by an STM tip. A rough estimate provided by the authors for the force applied to the flake by the tip was 500 pN for a typical flake of 4000 atoms. They also estimated that the tip displaces the flake initially by 2 Å corresponding to an energy of the order of 1 eV. Due to the nature of the experimental setup, this interaction is very difficult to characterise accurately and there is no guarantee of consistency between repeat experiments. The nature, magnitude, and duration of the force applied to the flake are not known. In addition, the graphitic substrate is also far from

perfect as it is in our simulations, which may impact the adsorption energy.

In our simulations we therefore used the smallest force necessary to consistently displace the flake from a commensurate position. The force was applied until the flake had moved 2 Å from its starting position, copying that done in these experiments. The minimum force required was found to be 0.06 kcal mol^{-1} Å^{-1} (4.2 pN) per atom or 150 kcal mol^{-1} Å^{-1} (10 nN) for the flakes we used, made of 2520 atoms. This is comparable to the value estimated in experiment (500 pN).

Below the minimum force of 0.06 kcal mol^{-1} Å^{-1} the flake stays in its commensurate position. The flake is heated up by the applied force and passes energy to the substrate, which subsequently also increases in temperature.

III. SIMULATIONS USING ESTABLISHED FORCEFIELDS

Simulations of flakes propelled on a graphite surface were also attempted with the established forcefields OPLS, AMBER, COMPASS and Dreiding. As stated in the main text they could not reproduce the experimentally observed behaviour of coming to rest and therefore these can not reproduce the temperature trend observed. The setup, equilibration and propulsion were identical to those described in the methods section with the exception of the forcefield parameters. The system used a graphite substrate at 1 K. At higher temperatures (100 K) the flake would not rest in a commensurate position: thermal fluctuations were enough to displace it even at these temperatures.

The flake remained in a superlubric state, travelling over 1000 nm in 10 ns without stopping, which means the friction (i.e. energy dissipation) in the system is inadequately represented by all the forcefields. Alignment events occurred with similar characteristics except that little energy was dissipated to the substrate.

IV. BOOTSTRAP SAMPLE SIZE

As reported in the methods section, a large ensemble of 180 replicas was undertaken to determine the distribution of results gained from this simulation and to arrive at the number of replicas needed to minimise uncertainties of reported averages. A histogram of straight-line distances travelled by flakes within this ensemble is shown in Figure S7a. How the

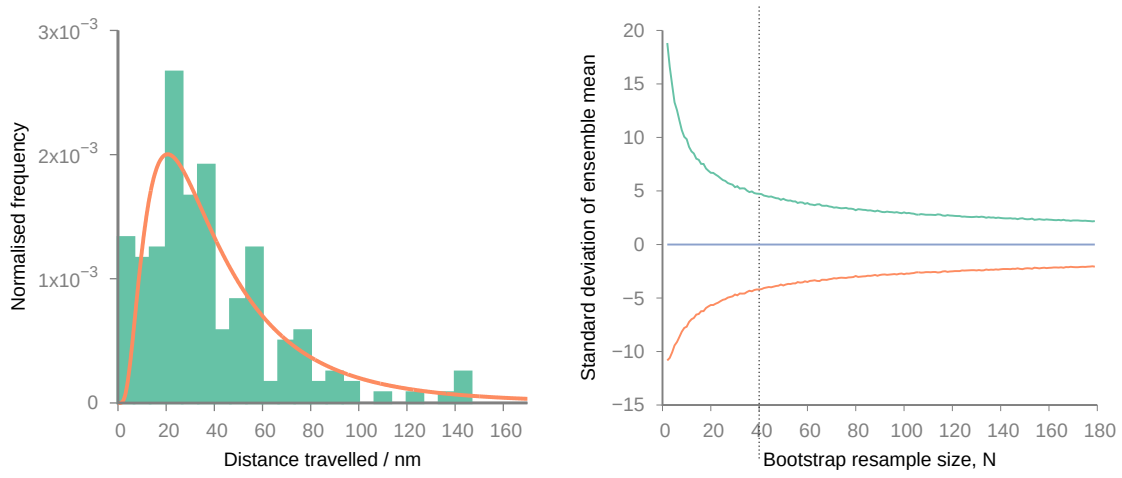

FIG. S7: (a) Distribution of distances travelled by graphene flakes following propulsion. This histogram has been taken from an ensemble of 180 replicas and fitted to a log-normal distribution. (b) The 68% confidence interval of averages obtained from different bootstrap resample sizes. We deem the point of diminishing returns to be at a sample size of 40 replicas; after this point adding more replicas makes little difference to the uncertainties.

confidence interval depends on resample size when using the bootstrap method[12] is shown in Figure S7b. $N = 40$ is indicated by a vertical dashed line; this is the size of ensemble (i.e. number of replicas we used in subsequent studies) that we concluded offers the best balance between computational efficiency and accuracy. The standard error with 40 replicas is +4.7/-4.2 nm.

V. DISCUSSION OF AVERAGE VALUES REPORTED

Values given in the main text for the distance travelled by a flake (e.g. Table I) are given as the arithmetic mean of the straight-line distance travelled. This is so that one can compare exactly with the experimental results and Feng *et al*'s averaging methods. However, for simulations we can also measure the total distance travelled, not just a straight line between start and end points, taking into account the changes in direction after alignment events. This was calculated by taking the sum of the straight-line distance travelled by the centre of mass of the flake every 5 ps. The total distance travelled gives a better indication of the friction between the substrate and projectile. Also, the geometric mean is a more representative average of a log-normally distributed population. Table S1 characterises the

same populations described in Table I in the main text, but using the geometric mean of the total distances travelled, which we believe to be the best representation of our data.

Temperature / K	Graphite substrate Distance / nm	Suspended Graphene Substrate Distance / nm
1	72.3 (+6.6/-6.0)	49.6 (+4.2/-3.9)
100	41.7 (+4.6/-4.2)	25.2 (+3.8/-3.3)
200	45.7 (+4.9/-5.5)	31.6 (+3.4/-3.0)

Temperature / K	15 × 15 nm Graphite Substrate Distance / nm	30 × 30 nm Graphite Substrate Distance / nm
1	72.3 (+6.6/-6.0)	64.5 (+3.4/-3.2)
100	41.7 (+4.6/-4.2)	24.5 (+4.0/-3.4)

TABLE S1: Geometric means of the total distance travelled by a 10 nm graphene flake on graphitic substrates. See Table I in the main text and surrounding text for a description of how these averages were developed.

For a comparison of how the using the total distance travelled changes the results compared to the straight line distance see Table S2, which shows the geometric averages of the straight line distance travelled.

Temperature / K	Graphite substrate Distance / nm	Suspended Graphene Substrate Distance / nm
1	54.2 (+5.7/-5.1)	40.1 (+3.9/-3.6)
100	25.2 (+4.2/-3.6)	19.1 (+3.2/-2.7)
200	30.5 (+5.0/-4.3)	20.0 (+2.7/-2.4)

TABLE S2: Geometric means of the straight-line distance travelled by a 10 nm flake.

Using the geometric averages in Table S1 indicates that the temperature trend — that flakes travel further at lower temperatures — observed in experiment is only a low temperature effect (<100 K). From 100 to 200 K we see a slight increase, although within error, in the distances travelled. The increased internal energy at higher temperatures of the flake and substrate mean the flake does not settle as quickly, increasing the distance travelled (i.e. towards the end of the flake's motion, at higher temperature it has more energy to move out of the defined commensurate potential energy well).

The distributions of the total distance travelled that formed the averages in Table S1 are shown in Figure S8. The distributions of the straight-line distances that formed the averages given in Table I and Table S2 are shown in Figure S9.

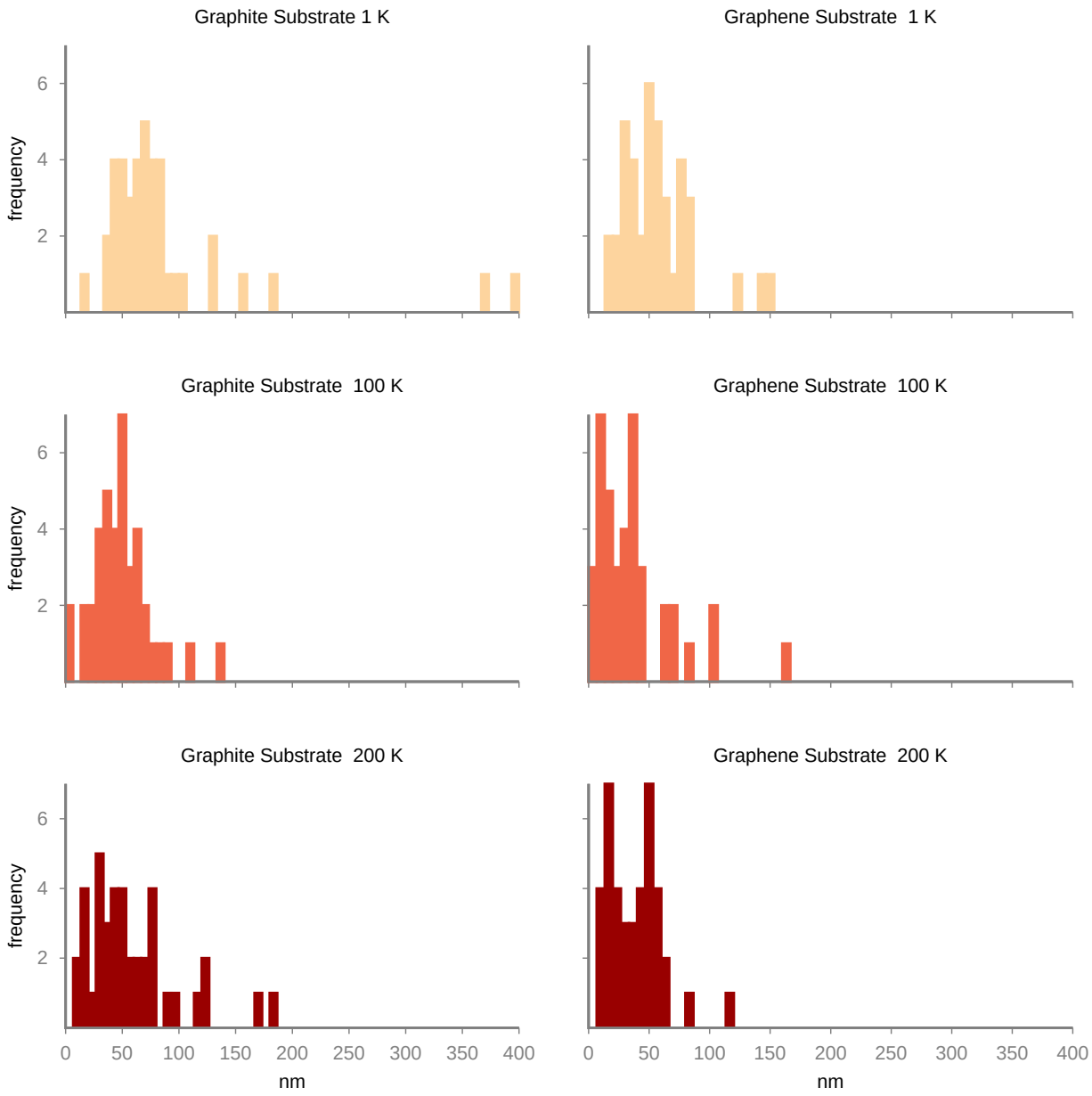

FIG. S8: Distributions of total distances travelled by a graphene flake after propulsion on different substrates. Two outliers in the 1 K graphite simulation do not disproportionately affect the overall temperature trend we observe. Including the outliers, the geometric mean is 72.4 nm; ignoring them, the mean is 66.8 nm.

VI. FLAKE-SUBSTRATE INTERACTION

In the main text we note that at higher temperatures the flake can loose energy due to the flake encountering out of plane atoms in the substrate caused by thermal fluctuations. This can be seen in figure S10 where in between alignment events the kinetic energy fluctuates

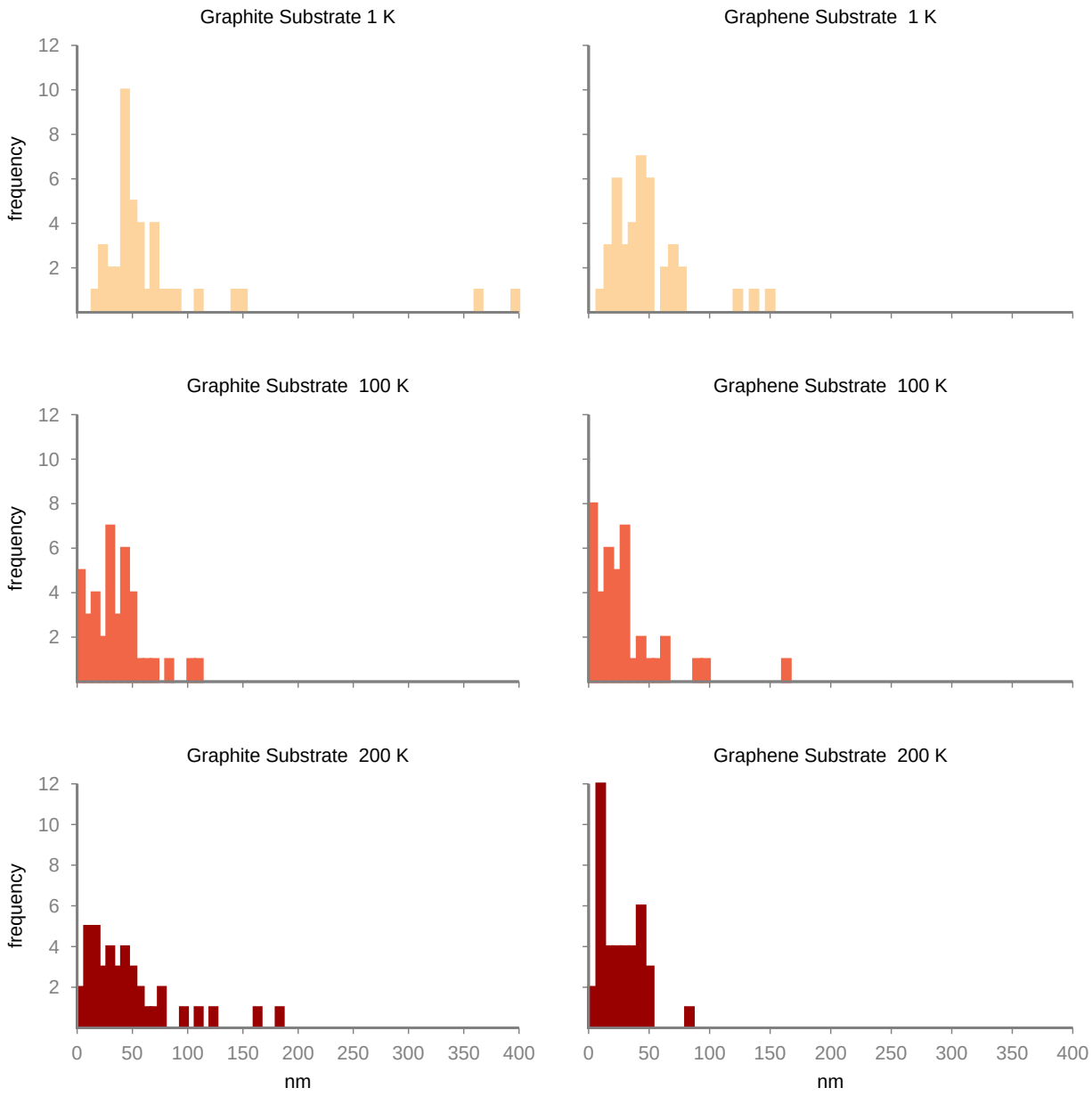

FIG. S9: Distributions of straight-line distances travelled by a graphene flake after propulsion on different substrates.

and decreases. The increased noise can be expected from the thermal fluctuations. The decrease in energy between events shows that energy is dissipated to the surface at higher temperatures in a different way than at lower temperatures.

In Figure 1b the translational and rotational energies were calculated between 5 ps intervals to reduce noise. Using a higher resolution (0.1 ps, see figure S11) makes the spikes in the interaction energy between the flake and substrate more visible as these are very fleeting

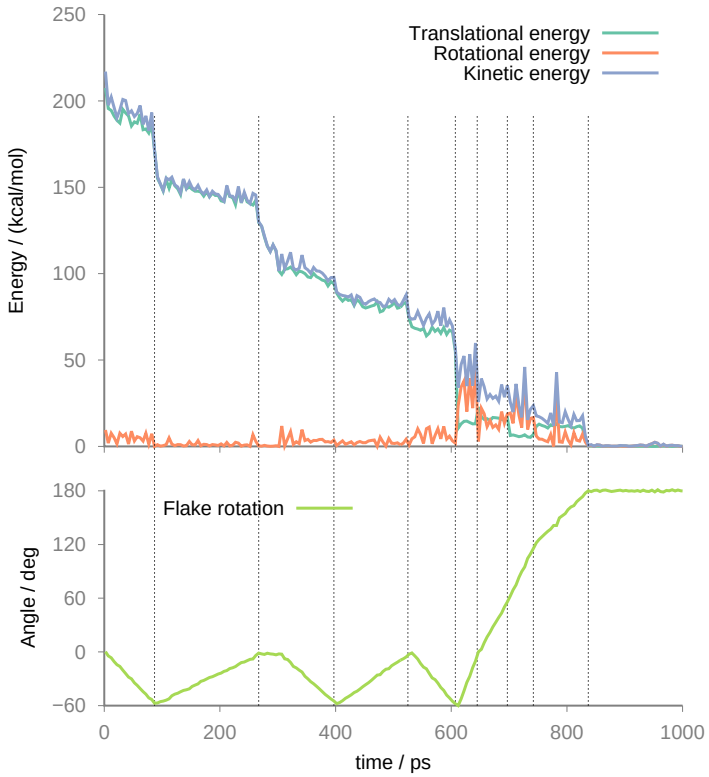

FIG. S10: Energies and orientation of a 10 nm graphene flake on a graphite substrate at 200 K. Alignment events have a similar effect as in the lower temperature simulation shown in Figure 1 but between alignments the energy decreases as the flake encounters thermal undulations in the substrate.

events. The higher resolution also gives a better indication of the energy dissipation to the substrate: the bond energy in the substrate jumps at each alignment event and steadily increases as energy is transferred from the flake.

VII. DEFLECTION HISTOGRAMS

The histograms shown in Figure 1d and 1e in the main text are a compilation of the deflection and energy loss caused by every alignment event in the large 180 replica ensemble.

The flake is said to be aligned if its orientation is within 10° of a multiple of 60°. The energy of a flake, E, is the sum of $T_{translational}$ and $T_{rotational}$. $E_{incident}$ is the energy of the flake when it first becomes aligned, $E_{deflected}$ is the energy immediately after or when the flake comes to a standstill. A point on the histogram is defined in polar coordinates: the

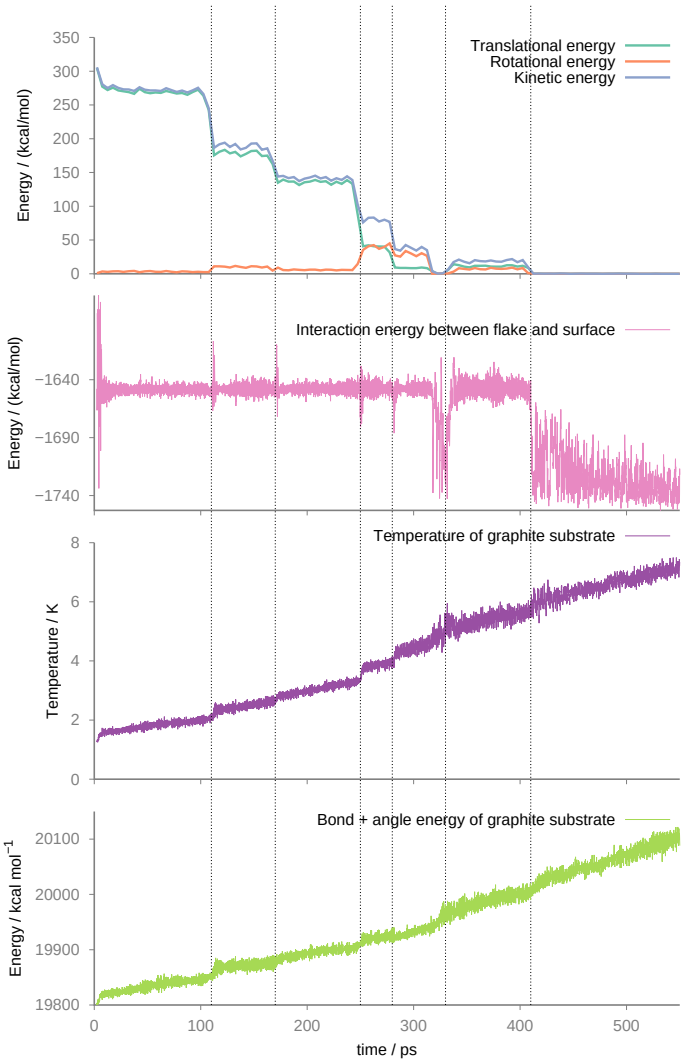

FIG. S11: Energies of a 10 nm flake on a graphite substrate at 1 K, the same trjaectory that is represented in Figure 1. The bottom 3 traces have a resolution of 0.1 ps.

angle is the deflection of the centre of mass trajectory during an alignment event and the the distance from the centre is $E_{deflected}/E_{incident}$.

Histogram bins are 0.067×0.067. The colour ranges from 0 counts (black) to 50 counts (white)

VIII. FINITE SIZE EFFECTS

In the main text, we report the results of the straight-line distance travelled for a graphene flake on a substrate of 15×15 nm^2 in size. To verify that the trends we observe are not influenced by finite size effects we repeated the simulations of 40 ensembles at 1 and 100 K

Temperature / K	15 × 15 nm Graphite Substrate Distance / nm	30 × 30 nm Graphite Substrate Distance / nm
1	68.8 (+12.8/-10.8)	58.8 (+4.2/-3.9)
100	35.4 (+4.1/-3.7)	27.5 (+4.9/-4.1)

TABLE S3: Size effect simulations to be compared with Table I in the main text.

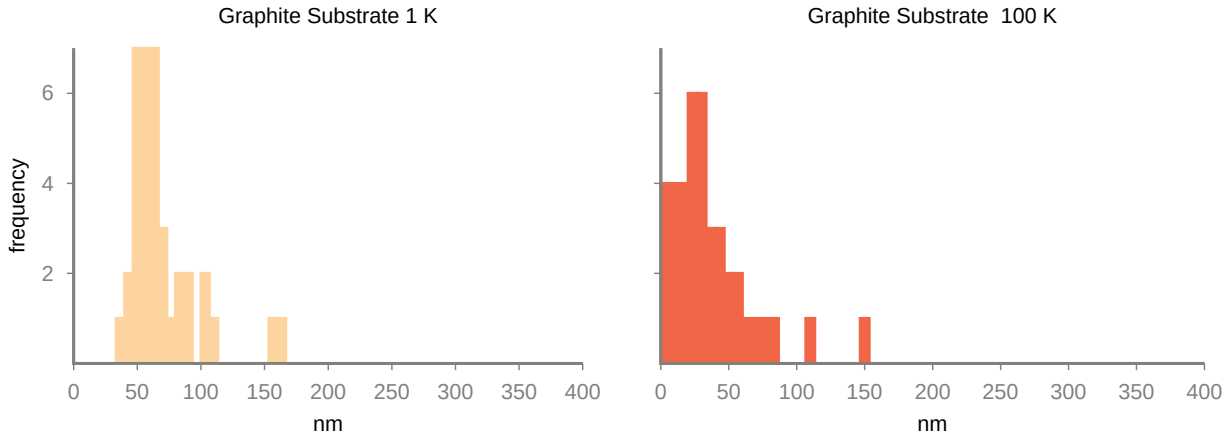

FIG. S12: Distributions of total distances travelled by a graphene flake after propulsion on a graphite substrate which is 30 × 30 nm.

with a graphite substrate using a much larger substrate of 30 × 30 nm^2, while keeping the size of the flake identical. As can be seen in Table S1 the temperature trend is preserved at the larger size and the distances travelled are of comparable value. There is some sensitivity to system size, which may be due to the presence of longer wavelength undulations, but this effect is within statistical error.

The distributions of distance travelled for the 30 × 30 nm^2 substrate are given in Figure S12.

IX. FOURIER TRANSFORMS

The Fourier transforms given in Figure 2 in the main text were calculated using the following method. The equilibrated starting coordinates for a replica were used, i.e. before the propulsion. The atoms in the top sheet of the graphite or all atoms in a graphene sheet were binned into a 50 by 50 array, with a bin size of 3 Å. The average z displacement from the sheet's centre of mass in each bin created the height function array to transform. A two-dimensional discrete fast Fourier transform spectrum of the array was calculated. The

amplitudes were obtained by dividing the spectral components along the x and y axis by the unit area of 2500. The x and y axes were used as these are the only truly periodic components of the spectrum. The amplitudes given in the Figure are the result of averaging the Fourier spectrum for all 40 replicas in each ensemble.

X. BEHAVIOUR OF A FLAKE ON A COMPRESSED SUBSTRATE

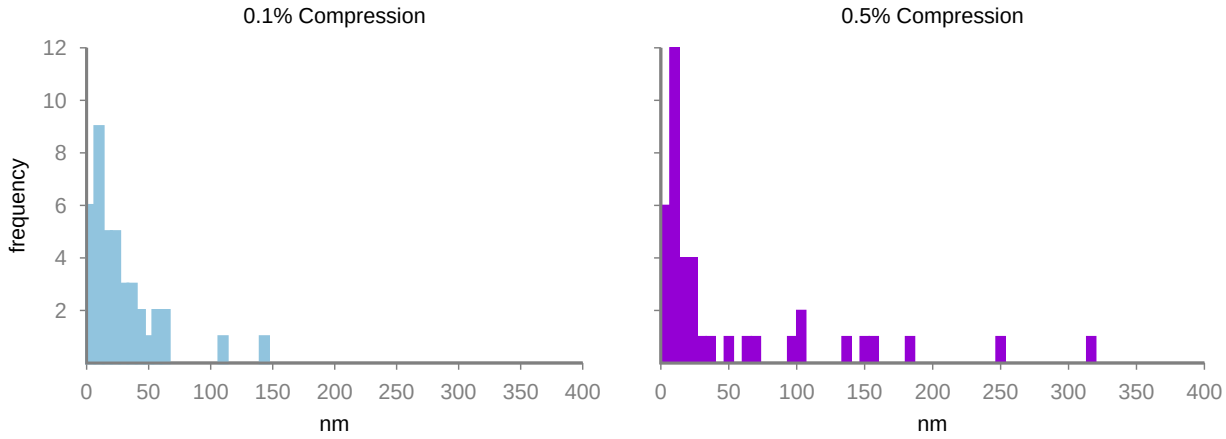

FIG. S13: Effect of compressing a graphene substrate on a flake's distance travelled after propulsion.

The distribution of distances travelled by a flake after propulsion on a compressed graphene substrate is different to that found in the simulations with a graphite substrate. The majority of flakes stop sliding shortly after propulsion, by the mechanism of interacting with undulations and ending in commensurate positions, as described in the main text.

However, a minority of flakes sit in the trough of a travelling wave in the substrate and are carried much further. A video of such an event is provided in Video 2. See the distributions of distances travelled for different substrate compressions in Figure S13 and Figure S14 for a description of the mechanism.

XI. COLLIDING FLAKES

The starting configuration was a single graphene sheet acting as the substrate 15 $\times$ 30 nm^2 in size held in place with a flat 12-6 Lennard-Jones potential acting as a wall at the

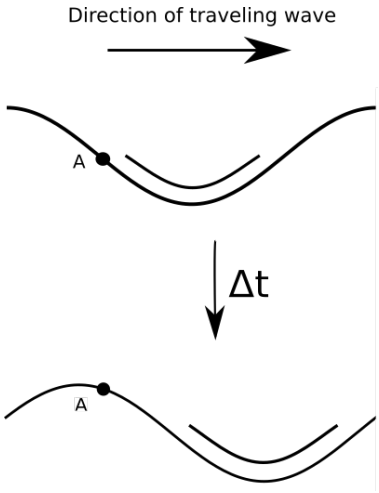

FIG. S14: A graphene flake trapped in the trough of a travelling wave formed in a suspended graphene sheet. Atom A only moves vertically and is initially on the leading edge of the travelling wave. As atom A moves up, between the two snapshots, it interacts repulsively with the flake. Therefore the flake is forced along the wave's direction. This effect is maximised when the flake's width is half the substrate's wavelength, as in this instance, as an atom on the trailing edge of the substrate wave will move down, and into a more attractive region of the interatomic potential. See also Video 2.

bottom of the simulation, as used before. Two 10 nm diameter flakes were arranged along the long axis, separated by 15 nm. The configuration was equilibrated at 1 K.

Pushing the flake with the same procedure described for the simulations testing the distance travelled, led to the propelled flake bouncing off the stationary one, while losing a small amount of energy.

Pushing a flake with the same force as before, 0.06 kcal $\mathrm{mol}^{-1}\mathring{A}^{-1}$ atom^{-1} but for 3.5 ps instead of 2.5 ps produced the simulation shown in Video 3. The propelled flake is flexible enough and has sufficient energy to climb on top of the stationary flake. While on top no alignment events take place, as discussed in the main text: the moving flake cannot align with the different substrates because they are AB stacked. The flake is propelled with significant force but does not dislodge the other flake.

XII. WHAM RESULTS

Figure S15 shows the results of a weighted histogram analysis[13], comparing the free energies associated with peeling and shearing mechanisms of exfoliation. The spring energy was divided by 2520 to make the quantity independent of size. The tolerance was 0.00001

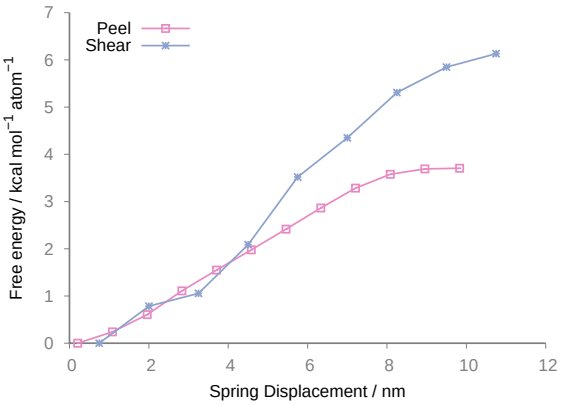

FIG. S15: Free energies per atom of exfoliating a graphene flake from a graphitic substrate via different mechanisms.

and number of Monte Carlo trials was 20.

A comparative steered simulation was carried out where the spring was moved 5 Å every 100 ps, resulting in an effected pulling speed of 5 m s^{-1}, instead of 1 m s^{-1}. The peeling mechanism required only 12 % less work. The reduced difference in work done is due to the sheered flake having less time to fall into commensurate positions along its exfoliation pathway, therefore less friction is observed between the flake and substrate. Nonetheless, this does show that the peeling mechanism remains favoured at different pulling speeds.

XIII. ACCOMPANYING VIDEOS

Video I: Trajectory of a flake pushed over a graphite substrate at 1 K. This is the same trajectory that is discussed in Figure 1 of the main text. Flake is 10 nm in diameter; the trajectory is of 418 ps duration.

Video 2: Trajectory of a flake 'surfing' in the trough of a travelling wave in a compressed graphene substrate; see Supplementary Discussion X. The substrate is coloured by its z coordinate: black represents valleys, white represents peaks. Any drift has been removed from the video, i.e. the coordinates have been shifted so the substrate does not move in the xy plane. The flake is 10 nm in diameter; the trajectory is of 684 ps duration.

Video 3: Flakes colliding, see section XI. Drift has been removed form the video as above.

Flakes are 10 nm in diameter; the trajectory is of 526 ps duration.

---

[1] Case, D. *et al. AMBER 2016.* University of California and San Francisco (2016).

[2] Jorgensen, W. L., Maxwell, D. S. & Tirado-Rives, J. Development and Testing of the OPLS All-Atom Force Field on Conformational Energetics and Properties of Organic Liquids. *Journal of the American Chemical Society* **118**, 11225–11236 (1996).

[3] Skountzos, E. N., Anastassiou, A., Mavrantzas, V. G. & Theodorou, D. N. Determination of the Mechanical Properties of a Poly(methyl methacrylate) Nanocomposite with Functionalized Graphene Sheets through Detailed Atomistic Simulations. *Macromolecules* **47**, 8072–8088 (2014).

[4] Sun, H. COMPASS: An ab Initio Force-Field Optimized for Condensed-Phase ApplicationsOverview with Details on Alkane and Benzene Compounds. *The Journal of Physical Chemistry B* **102**, 7338–7364 (1998).

[5] Wang, Z., Selbach, S. M. & Grande, T. Van der Waals density functional study of the energetics of alkali metal intercalation in graphite. *RSC Advances* **4**, 3973–3983 (2014).

[6] Zacharia, R., Ulbricht, H. & Hertel, T. Interlayer cohesive energy of graphite from thermal desorption of polyaromatic hydrocarbons. *Physical Review B* **69**, 155406 (2004).

[7] Liu, Z. *et al.* Interlayer binding energy of graphite: A mesoscopic determination from deformation. *Physical Review B* **85**, 205418 (2012).

[8] Benedict, L. X. *et al.* Microscopic determination of the interlayer binding energy in graphite. *Chemical Physics Letters* **286**, 490–496 (1998).

[9] Shih, C.-J., Lin, S., Strano, M. S. & Blankschtein, D. Understanding the Stabilization of Liquid-Phase-Exfoliated Graphene in Polar Solvents: Molecular Dynamics Simulations and Kinetic Theory of Colloid Aggregation. *Journal of the American Chemical Society* **132**, 14638–14648 (2010).

[10] Suter, J. L., Groen, D. & Coveney, P. V. Mechanism of Exfoliation and Prediction of Materials Properties of ClayPolymer Nanocomposites from Multiscale Modeling. *Nano Letters* **15** (2015).

[11] Gao, W. & Tkatchenko, A. Sliding Mechanisms in Multilayered Hexagonal Boron Nitride and Graphene: The Effects of Directionality, Thickness, and Sliding Constraints. *Physical Review*

Letters **114**, 096101 (2015).

[12] Efron, B. & Tibshirani, R. J. *An introduction to the bootstrap* (CRC press, 1994).

[13] Grossfield, A. Wham: the weighted histogram analysis method (2014). Http://membrane.urmc.rochester.edu/content/wham.